# Estimating Tropical Pacific Rainfall Using Digital Satellite Data

CRAIG E. MOTELL AND BRYAN C. WEARE

*Department of Land, Air and Water Resources, University of California, Davis, CA 95616*

(Manuscript received 4 November 1986, in final form 28 April 1987)

ABSTRACT

Statistical models that estimate tropical Pacific rainfall from the National Oceanic and Atmospheric Administration's global archive of polar-orbiter satellite data have been derived and tested. These rainfall models are based on the assumptions that rainfall is linearly related to bright visible and cold infrared radiation (IR) satellite irradiances. The models were derived by using measured monthly rainfall from small, flat, tropical islands with elevations less than 30 m together with digital IR and visible satellite data.

Three models were derived: one used visible and nighttime IR data (NIRVISQ); the second used only visible data (VISQ); and the third used an average of daytime and nighttime IR data (AVEIR). These models were found to predict between 62% and 67% of the variance of 1051 station-months of hindcast rainfall data measured from June 1974 through mid-March 1978 (J74M78). However, rainfall was found to be underpredicted on relatively high mean rainfall islands and vice versa. Similar prediction accuracies were found when the rainfall models were used to estimate rainfall on new low-latitude island stations during the J74M78 period. All three models showed a decrease in predictive skill during time periods after J74M78.

Tropical Pacific annual rainfall maps, estimated using the rainfall models and satellite data from June 1974 through May 1977, showed that NIRVISQ and VISQ may greatly overpredict rainfall in regions where stratus clouds are common such as in the eastern Pacific Ocean, but AVEIR appeared to predict reasonable rainfall amounts throughout the tropical Pacific. The AVEIR is thus the preferred model for predicting tropical oceanic rainfall.

## 1. Introduction

In recent years numerous researchers have used the National Oceanic and Atmospheric Administration's (NOAA) global archive of mesoscale-resolution, polar-orbiter, satellite radiation data (Gruber and Winston, 1978) to make qualitative inferences of tropical convective activity (Heddinghaus and Krueger, 1981; Riehl and Miller, 1978) and precipitation (Short and Wallace, 1979).

Despite this extensive use, only a few attempts have been made to quantitatively relate these data to rainfall rates. One such attempt was that of Lau and Chan (1983) who used NOAA's 2.5° resolution archived infrared radiation (IR) data to study short-term climate variability. Relating this data to microwave estimates of tropical Pacific rain rates during May 1974–February 1975 (Rao et al., 1976), Lau and Chan derived the linear equation $R = 0.05 + 66.7N_c$, where $R$ is the rainfall rate in millimeters per month and $N_c$ is the number of days in a month in which the grid point daily IR average falls below a threshold of 240 W m$^{-2}$. Verification of the method with new data was not attempted.

Kilonsky and Ramage (1976) used daily visible mosiacs from the same NOAA satellites to derive a regression equation which relates monthly Pacific atoll rainfall to the frequency of highly reflective clouds ($F_c$). Their regression equation, $R = 55.3 + 39.2F_c$, accounts for approximately 56% of the variance in the monthly island rainfall dataset used in their study.

Garcia (1981) used Kilonsky and Ramage's satellite method to make rainfall estimates for the Atlantic GATE study area. He then compared these results with high-resolution geostationary satellite IR-based rainfall estimates derived by the Griffith-Woodley method (Woodley et al., 1980), and found that for the entire GATE period (27 June through 20 September 1974) there was a 0.92 correlation between the two methods. Both these procedures yielded rainfall volume estimates which were within 15% of the ship radar estimates (Garcia, 1981). Although Garcia's results support Kilonsky and Ramage's method, this method has the disadvantage of requiring time-consuming subjective analysis of the visible mosiacs to make rainfall estimates.

The present paper attempts to further quantify the relationship between NOAA-archived digital satellite data and tropical Pacific convective rainfall. Following Kilonsky and Ramage, we assume that rainfall measured on small tropical islands is representative of oceanic rainfall (Dorman, 1982). Using satellite data for a station location, regression equations relating rainfall to satellite radiation measurements are derived; thereafter, the regression equations are verified using new data. Finally, sample tropical Pacific rainfall estimates are shown and discussed.

## 2. Data

Measurements made by NOAA operational polar-orbiting satellites have been archived in a convenient, standardized format since June 1974 (Gruber and Winston, 1978). Archived components consist of global outgoing IR, incoming visible, and absorbed visible radiation measurements. The planetary albedo is derived from incoming and reflected visible radiation measurements, while the IR archive consists of both daytime and nighttime measurements.

### *a. Satellite data*

Archived radiational components are formed by averaging together high-resolution satellite observations to form a medium-resolution hemispheric dataset (125 × 125 square array) aligned with the National Meteorological Center polar sterographic map base. The grid spacings vary in size from ~102 km at the equator to ~204 km near the poles. A supplementary 2.5° latitude–longitude global data array is derived by a bilinear interpolation of the medium-resolution dataset.

The satellites and methods used to form these archived datasets have, by necessity, undergone several changes since 1974. Different types of satellites have been used, orbits and instrumentation have varied, and data reduction procedures modified. Highlights of these changes are given in Table 1.

The changes in the satellites and methods used to obtain and interpret the satellite data influence the homogeneity of the archived data. Due to the diurnal nature of cloudiness (Hunt, 1981), changing equatorial crossing times—and hence satellite observation times—influence even long-term estimates of albedo and outgoing IR (Gruber and Krueger, 1984). For example, Figs. 1a, b show average monthly albedo and IR for the Pacific Basin (30°N to 30°S and 110°E to 70°W) with equatorial crossing time changes denoted with dashed vertical lines. Noticeable features include a decreasing trend in annual albedo from June 1974 through mid-March 1978, and relatively large albedo values during the NOAA-6 period. It will be shown that our model, which uses only an albedo specifier, predicts an 11% increase in mean rainfall for the unusually high 1980–81 observations with a 0730 LST crossing time. Smaller apparent irregularities in the IR data are also potentially significant. Our rainfall prediction model that uses IR data is such that the approximate 2.5 W $m^{-2}$ difference between the means of the 1974–78 and the 1980–81 periods lead to changes of about 9% in predicted rainfall.

It should also be noted that IR values prior to 1 March 1983 were found to have a positive bias of approximately 13 W $m^{-2}$ relative to the broadband measurements of the Earth Radiation Budget sensors flown on the NIMBUS-7 satellite (Gruber and Krueger, 1984). Equations given in the appendix of Gruber and Krueger can be applied to the archived data to standardize the IR values and to remove the positive bias in the data. These equations were not applied to data described in the body of this paper.

### *b. Island data*

Monthly tropical Pacific rainfalls measured on small, relatively flat islands, were obtained from data supplied by John Horel (Horel, 1982). Measured rainfall from these islands is assumed to be representative of oceanic rainfall. The database consists of monthly rainfall from 62 island stations (Fig. 2) for the period 1974–80; max-

TABLE 1. Summary of polar-orbiter satellite sensors, high-resolution data and archived low-resolution data.

| | NOAA SR series* | TIROS-N | NOAA-6 | NOAA-7, 8, 9 |
|---|---|---|---|---|
| Sensor | two-channel SR | four-channel† AVHRR | four-channel AVHRR | five-channel AVHRR |
| Channels | 0.5–0.7 μm VIS‡<br>10.5–12.5 μm IR@ | 0.55–0.90 μm VIS<br>10.5–11.5 μm IR | 0.58–0.68 μm VIS<br>10.5–11.5 μm IR | 0.58–0.68 μm VIS<br>11.5–12.5 μm IR |
| Operation dates | 1 June 1974–16 Mar. 1978 | 1 Jan. 1979–20 Jan. 1980 | 22 Feb. 1980–30 Aug. 1981# | 1 Sept. 1981–Present |
| Equatorial crossing times | 0900–2100 | 0330–1530 | 0730–1930 | 0230–1430 |
| Resolution | VIS 4 km<br>IR 8 km | VIS 1 km<br>IR 4 km | VIS 1 km<br>IR 4 km | VIS 1 km<br>IR 4 km |
| | | *Archived data* | | |
| | | 125 × 125 hemispheric dataset | Degree dataset | |
| Resolution | | 102 km at equator, 204 km at poles | 2.5° latitude, longitude grids | |

* Scanning radiometer radiation sensor.
† Advanced very high resolution radiometer sensor. Only two of sensor's channels are used to form digital data archive.
‡ Measured window reflected visible radiation.
@ Measured window outgoing longwave radiation.
# IR measurements were achieved beginning 22 Feb. 1980. VIS measurements were archived beginning on 2 May 1980.

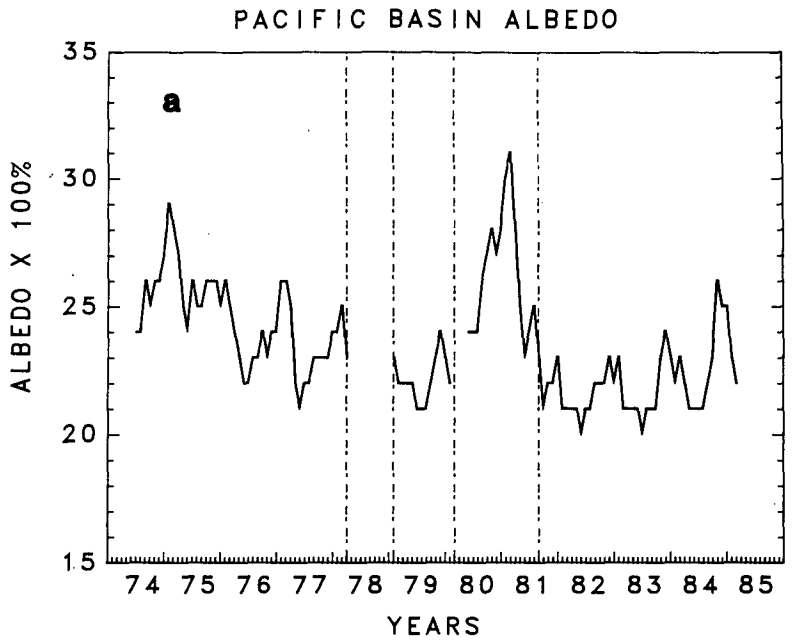


FIG. 1a. Average monthly albedo, in percent, for the Pacific basin (110°E, 30°S to 70°W, 30°N) 2.5° × 2.5° albedo dataset. The vertical dashed lines represent changes in satellite equatorial crossing times.

imum elevations on 44 islands are less than 30 m (98 ft). Appendix A lists the locations and heights of the islands whose data were used.

The 44 low-elevation islands were divided into two groups: the first, the "development" dataset, was used in deriving the regression equations relating satellite observations to surface rainfall; the second, the "verification" dataset, was used for verifying the regression equations on independent data. A third "secondary" dataset was formed using rainfall data from the re-

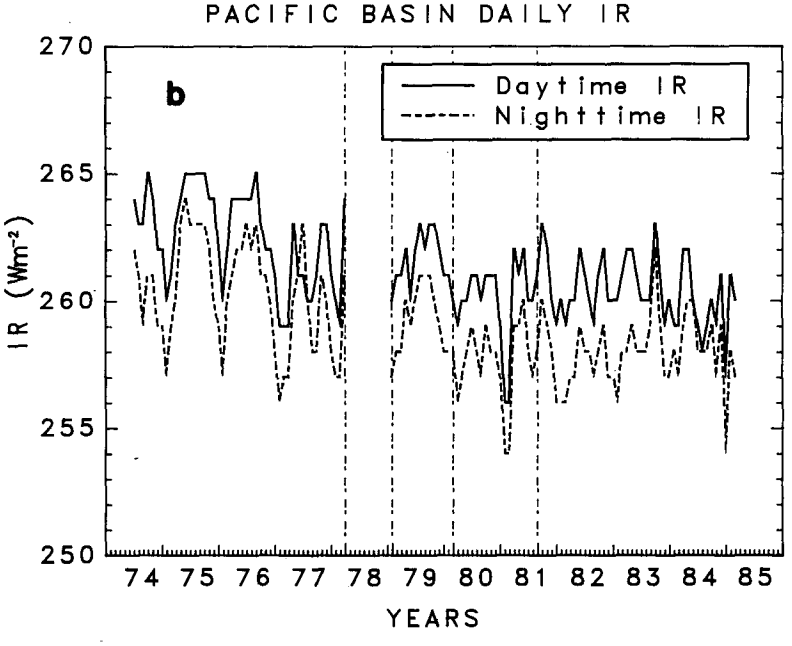


FIG. 1b. As in Fig. 1a except for daytime IR (thick solid line) and nighttime IR (thick dashed line).

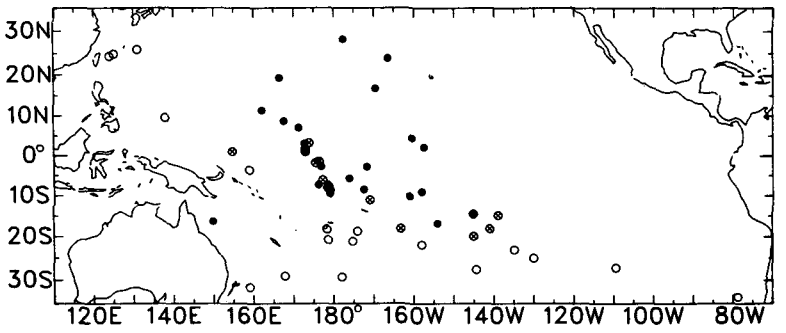


FIG. 2. Locations of island rainfall stations used in this study. Stations of the development dataset are denoted by closed circles, those of the verification dataset by circles with crosses, and those of the secondary dataset by open circles.

maining higher-elevation islands. Because of possible large local orographic influences, the secondary dataset was used for qualitative verification of the regression equations only.

## 3. Model development

The purpose of this study was to develop accurate, stable statistical models to specify monthly tropical Pacific rainfall from NOAA polar-orbiting data. The predictor variables chosen were constrained by the spatial and temporal resolution of the NOAA data. Radiation values over each island were derived by bilinear interpolation of archived radiation components to the island's position. These interpolated values were used to form predictor variables, after which island rainfall was fitted, using least-squares, to these predictors to form regression equations for each island. Those predictors which singly showed the highest correlation to rainfall were combined to form multiparameter regression equations. These multiparameter equations were again compared to determine which predictor combinations had the highest correlations to individual island rainfall. Subsequently, all island rainfalls were pooled to form one general population of rainfall data. The pooled rainfall data were then fitted to a final set of predictor variables to form general regression equations.

Two types of satellite-derived predictor variables were chosen: monthly mean and mean threshold radiation.

### *a. Monthly mean radiation*

Rainfall from each development station was compared to mean daytime IR (DIR), mean nighttime IR (NIR), and mean albedo (VIS) by forming correlation coefficients between monthly values of radiation and rainfall for the period June 1974–December 1980. At each station, the coefficients were significant at the 0.01 level. Mean correlations, formed by combining station correlations weighted by the number of observations per station (Brooks and Carruthers, 1953) of 0.71, −0.76 and −0.74 for VIS, DIR and NIR, respectively, suggest nearly identical skill for all three predictors.

Residual errors were examined using a linear regression equation fitting rainfall to the mean predictors. Rankin plots of the residuals showed that normality could be assumed for the errors (Weisberg, 1980). Residuals plotted against rainfall magnitude showed that most islands had rainfall that was linearly related to mean radiation. These statistics lead to a reasonable assumption that rainfall is linearly related to mean IR or albedo.

### *b. Monthly mean threshold radiation*

Many published satellite data-based rainfall prediction schemes assume some IR or albedo pixel value which, when exceeded, maximizes the correlation with concurrent rainfall. (Barrett and Martin, 1981, reviews these techniques.) For example, Stout et al. (1979) assumed that any cloud colder than 247 K or with an albedo greater than 45% was likely to produce precipitation within 30 min.

The threshold statistics used in this paper differ from those used in previous studies in two major respects. First, thresholds are selected to predict monthly rainfall, rather than hourly or daily rainfall (Stout et al., 1979); second, the threshold statistics are defined as the difference between an observed value and a chosen threshold. The basis for using this type of threshold statistic is the assumption that the colder or brighter a cloud is, the more rain it will produce. Differences between observed and threshold values are summed over a month and normalized by dividing by the number of observations during that month ($N$). The IR and albedo radiation threshold predictors are formed by the following equations:

$$\left.\begin{aligned} \mathrm{IRQ} &= \Big[\sum_{i=1}^{N} (\mathrm{IR}_c - \mathrm{IR}_i) I_i\Big] N^{-1} \\ \mathrm{VISQ} &= \Big[\sum_{i=1}^{N} (\mathrm{VIS}_i - \mathrm{VIS}_c) I_i\Big] N^{-1} \end{aligned}\right\}, \qquad (1)$$

where IR is the measured day or night IR, VIS the measured albedo, subscript $c$ indicates the respective threshold value, and $I$ is an indicator variable defined by the equation

$$I = \begin{cases} 0 & \text{when } IR_c \leq IR \text{ or } VIS_c \geq VIS. \\ 1 & \text{when } IR_c > IR \text{ or } VIS_c < VIS. \end{cases}$$

The day IRQ statistic is denoted as DIRQ and the night as NIRQ.

To determine the ability of different thresholds to predict rainfall, correlations between observed and predicted rainfall were examined for the development stations using different threshold levels. Table 2 lists the mean correlations for a selected range of daily and nightly IR and albedo thresholds. The most notable feature of Table 2 is the wide range of thresholds which have nearly identical correlations. In fact, all DIRQ and NIRQ thresholds above 130 W $m^{-2}$ are significantly correlated to rainfall at the 0.01 level. The insensitivity of correlation values to threshold levels has been shown by others (Arkin, 1979). The optimum infrared correlations, associated with thresholds ranging from 260–280 W $m^{-2}$ for DIRQ and 245–285 W $m^{-2}$ for NIRQ, have values of 0.77 and 0.75, respectively. The magnitude of these correlations are not significantly larger than the correlations of −0.76 and −0.74 for the mean DIR and NIR predictors, respectively.

The VISQ threshold also shows a wide range of statistically significant thresholds. All thresholds below 75% are significant at the 0.01 level. The optimum VISQ correlations range from 20%–35% albedo with a value of 0.78, compared to the 0.71 correlation value for the mean predictor. The difference between the correlation magnitudes for threshold and mean albedo predictors is somewhat larger than in the case of IR predictors, yet it is still not significant at the 0.05 level.

### c. *Multiparameter model selections*

A sample of threshold predictors were combined into multiparameter regression equations, using two or three parameter combinations of albedo and IR thresholds. When the threshold predictors were combined, IR thresholds slightly below the optimum threshold ranges, near 250 W $m^{-2}$, and albedo thresholds near 35%, seemed to predict rainfall with the greatest accuracy (correlation). Thus, the results of subsection 3b served as a starting point, and reanalysis was undertaken to determine which threshold levels work best in multiparameter models.

TABLE 2. Summary of mean correlations for different threshold levels and radiation parameters, derived from the development island stations.

| IR level (W $m^{-2}$) | DIR | NIR | Albedo × 100 | VIS |
|---|---|---|---|---|
| 190 | 0.70 | 0.69 | 15 | 0.76 |
| 200 | 0.71 | 0.70 | 20 | 0.78 |
| 210 | 0.73 | 0.72 | 25 | 0.78 |
| 220 | 0.74 | 0.73 | 30 | 0.78 |
| 230 | 0.75 | 0.74 | 35 | 0.78 |
| 240 | 0.76 | 0.74 | 40 | 0.77 |
| 250 | 0.76 | 0.75 | 45 | 0.74 |
| 260 | 0.77 | 0.75 | 50 | 0.71 |
| 270 | 0.77 | 0.75 | 55 | 0.68 |
| 280 | 0.77 | 0.75 | 60 | 0.64 |
| 290 | 0.76 | 0.74 | 65 | 0.58 |

If one considers the possible combinations of regression equations with different threshold predictors ranging from 240–290 W $m^{-2}$ for IR and 20%–35% for albedo, in five-unit increments, the total number is 2300. Therefore, a subjective method was used to reduce the number of possible predictors.

Predictor variables were chosen based upon the type of predictor and preliminary analysis on different threshold combinations. Mean predictors were chosen as one type of predictor, leaving only a choice of which threshold levels to use. Fifteen combinations of threshold levels for DIR, NIR and VIS statistics were analyzed. After comparing correlations between predicted and observed rainfall, the following conclusions were made. The accuracy of the regression equations seemed to be relatively insensitive to the thresholds chosen when these thresholds were near the optimum thresholds shown in Table 2; however, DIR and NIR thresholds of ~250 W $m^{-2}$ used with albedo thresholds of ~35% appear to give the highest predicted-observed rainfall correlations. Changing the threshold levels in the given range resulted only in nonsignificant mean correlation changes ($r = \sim 0.75 \pm 0.02$) in the regression equations sampled. Therefore, further analysis was not considered useful.

Thus, three threshold statistics were chosen for further analysis. These three predictors, along with the mean predictors, make up the final set of possible rainfall predictors and are summarized below:

1) 250 W $m^{-2}$ DIRQ,
2) 250 W $m^{-2}$ NIRQ,
3) 35% VISQ,
4) DIR mean,
5) NIR mean,
6) and VIS mean.

Regression equations using a subset of the above predictors will never produce higher hindcast predicted–observed rainfall correlations or lower root-mean-square errors (rmse) than the full set of six predictors. On the other hand, equations using a subset of the above six predictors may predict rainfall with higher correlation and lower rmse on forecast data (Daniel and Wood, 1980). Forecast data are defined as any data that are not used in determining the regression parameters. To prevent "overfitting" of the hindcast data by a multiparameter regression equation, unimportant variables should be eliminated.

With six predictors there are $2^6$ or 64 combinations of regression equations that should be examined. A common fallacy is to assume stepwise regression techniques will yield the best prediction equation. Unfortunately, stepwise regression can lead to confusing results when the predictor variables are highly correlated, and additionally, stepwise schemes assume that there is one best equation rather than several equally good equations.

The most comprehensive approach is to compare all 64 regression equations. For comparing combinations of predictors, some statistic must be chosen as a criterion to maximize or minimize; for this study the adjusted coefficient of determination ($R^{2p}$) was chosen. This is defined as

$$R^{2p} = 1 - [(N-1)/(N-p)](1-R^2), \quad (2)$$

where $N$ is the number of observations, $p$ the number of predictors (at most six in this case), and $R^2$ the coefficient of determination. Equations with the largest $R^{2p}$ value should predict rainfall with the greatest accuracy when using forecast data (Weisberg, 1980).

The advantage in using the $R^{2p}$ instead of the simple $R^2$ can be seen from Eq. 2, which shows that increasing the number of predictors, $p$, may serve to actually lower the $R^{2p}$. In contrast, $R^2$ can never be lowered by adding predictors. For this reason, the $R^{2p}$ statistic may select a simpler model over a more complex model.

In order to select a set of optimum regression models applicable to any part of tropical Pacific, concurrent rainfall and satellite data from the development stations from June 1974 through mid-March 1978 were pooled together to form a "pooled" rainfall and satellite dataset. This pooled dataset was used to derive $R^{2p}$ values. Table 3 shows the $R^{2p}$ values associated with the most skillful predictors for one through four parameter models. This table shows that the $R^{2p}$ values are not increased by having more than two predictors, suggesting that two-parameter models will predict rainfall as well as models using more than two predictors.

The VISQ model appears to be the best one-parameter model, while the two best two-parameter models are formed from a combination of either NIRQ or NIR and the VISQ statistics. The probable reason for the inclusion of the night IR and albedo predictors in the two parameter models is that these predictors are observed to have lower correlations between each other than any other two statistics. It is expected that any model using a minimum number of predictors will use those with the most independent amount of information, such as NIR or NIRQ and VISQ which are formed from measurements taken 12 h apart and at different wavelengths.

TABLE 3. The $R^{2p}$ values for different predictor combinations and predictor number.

| $R^{2p}$ | Predictors | Predictor number |
|---|---|---|
| 0.63 | VISQ | 1 |
| 0.61 | DIR | 1 |
| 0.61 | DIRQ | 1 |
| 0.67 | NIR & VISQ | 2 |
| 0.67 | VISQ & NIRQ | 2 |
| 0.65 | DIR & VISQ | 2 |
| 0.67 | NIR & VISQ & NIRQ | 3 |
| 0.67 | NIR & DIRQ & VISQ | 3 |
| 0.67 | DIR & NIR & VISQ | 3 |
| 0.67 | DIR & DIRQ & VISQ & NIRQ | 4 |
| 0.67 | NIR & DIRQ & VISQ & NIRQ | 4 |
| 0.67 | VIS & NIR & VISQ & NIRQ | 4 |

Thus, statistical analysis of the pooled data indicates that the best one-parameter model uses an albedo predictor with a threshold of 35%. The best two-parameter models use the same albedo threshold with either a mean night IR predictor or a night IR threshold predictor with a threshold of 250 W $m^{-2}$. More complicated models using more predictors were not found to raise $R^{2p}$.

### *d. Derivation of the rainfall models*

Based upon the previously described analyses, three variables were selected as possible rainfall predictors. Additionally, a fourth variable, (AVEIR), derived by averaging day and night IR observations to form an average monthly predictor, was chosen for comparison with other studies that commonly use such daily IR averages (Heddinghaus and Krueger, 1981).

From the pooled data, the following regression equations were derived by least-squares as the best one- and two-parameter equations:

model VISQ:

$$R = 52.494 + 4.309\,(\text{VISQ}), \quad (3)$$

model NIRVISQ:

$$R = 812.034 - 2.736\,(\text{NIR}) + 2.600\,(\text{VISQ}), \quad (4)$$

model NIRQVISQ:

$$R = 44.192 + 0.481\,(\text{NIRQ}) + 2.590\,(\text{VSQ}), \quad (5)$$

model AVEIR:

$$R = 1763.847 - 6.107\,[(\text{DIR} + \text{NIR})/2]. \quad (6)$$

The predictors are defined as before, and $R$ is the satellite-predicted rainfall calculated in units of millimeters per month. An indicator variable is included in these models which sets rainfall to 0 mm if rainfall is predicted to be negative (sometimes occurring over regions like the Australian desert). Appendix B shows equations corresponding to Eqs. 4 and 6 based upon infrared data adjusted in the manner proposed by Gruber and Krueger (1984).

The regression statistics associated with the rainfall prediction models are shown in Table 4. The correlations ($r$) suggest that the two-parameter models are

TABLE 4. Statistical summary for rainfall prediction models.

| Model | $r$ | rmse | Degrees of freedom |
|---|---|---|---|
| VISQ | 0.79 | 92.5 | 1049 |
| NIRVISQ | 0.82 | 87.6 | 1048 |
| NIRQVISQ | 0.81 | 88.0 | 1048 |
| AVEIR | 0.79 | 93.5 | 1048 |

slightly better than either the one-parameter VISQ model, or the AVEIR model. The NIRVISQ and NIRQVISQ models show nearly identical correlations and root-mean-square errors (rmse), which suggest that the night IR threshold and mean predictors predict rainfall equally well. Because rainfall prediction does not appear to be improved by using the threshold night IR predictor, further analysis will include only the use of the mean night IR predictor—NIR.

## 4. Verification of the rainfall prediction models

The verification analysis in this study was divided into three steps. First, the regression equations derived from pooling data from the 24 islands of the development dataset during the period June 1974–mid-March 1978 (J74M78) were used to predict rainfall on the individual islands. Second, the equations were used to predict rainfall with new spatial data using the verification and secondary datasets. Third, the equations were used to predict rainfall for new time periods using data later than March 1978.

### *a. Testing using the development data*

The rainfall models were formed by pooling data from all the development stations. As a result, the correlation between an observed station's rainfall and predicted rainfall will be less than if the regression equation used was formed using only data from that island. Therefore, to test these regression models, $r$ and rmse were derived using predicted rainfall at individual developmental stations. All development island station correlations were still found to be significant at the 0.01 level. Mean station correlations for these stations are summarized in Table 5.

Unfortunately, the regression equations formed using the pooled data appear to frequently over- or underpredict rainfall at individual islands. The bias in the rainfall estimates is quantified by defining the bias as the mean difference between the predicted ($R_p$) and observed ($R_0$) rainfall, calculated by the formula

$$\text{BIAS} = [(R_0 - R_p)]N^{-1}, \tag{7}$$

where $N$ is the number of months. Figure 3 shows a plot of bias versus average monthly island rainfall for the AVEIR model. Rainfall generally appears to be overpredicted on relatively low mean rainfall stations and underpredicted on relatively high mean rainfall stations. Similar results are found with the other two models.

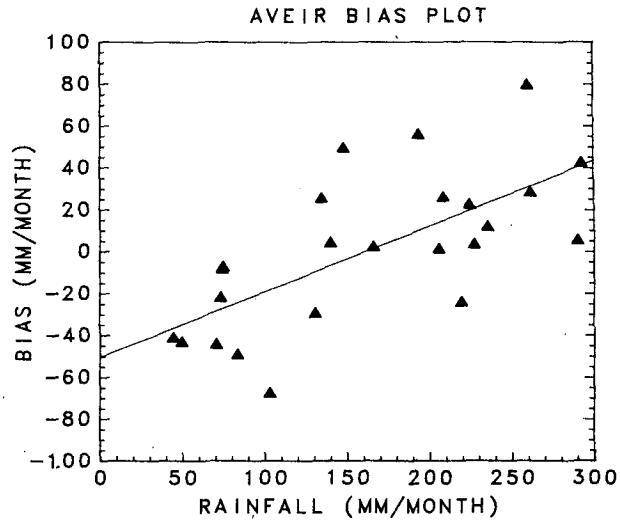


FIG. 3. Scatter plot showing the bias (mm month$^{-1}$) in rainfall predicted by the AVEIR model versus average monthly rainfall for the period June 1974–mid-March 1978.

In order to estimate the influence of these biases, rainfall anomalies were formed for both observed and predicted rainfall. An observed mean for each station was calculated for the period June 1974–March 1978. Observed anomalies were then calculated as the differences between observed monthly values and these means. Predicted anomalies were formed using one of the models AVEIR, NIRVISQ or VISQ to predict long-term mean rainfall for the same period at each island; predicted deviations from this long-term mean formed the satellite-predicted anomalies. The rmse for each model is 6%–9% lower for the anomalies than for the totals, indicating that the bias is responsible for an appreciable part of the rainfall prediction error.

TABLE 5. Mean correlations ($r$) and rmse derived from the development and verification datasets for the period June 1974–mid-March 1978. The number of station-month observations (obs) is also given.

| | Development data | | | Verification data | | |
|---|---|---|---|---|---|---|
| Model | $r$ | rmse | obs | $r$ | rmse | obs |
| VISQ | 0.76 | 84.6 | 1051 | 0.75 | 89.6 | 431 |
| NIRVISQ | 0.78 | 80.2 | 1051 | 0.81 | 81.1 | 428 |
| AVEIR | 0.74 | 87.3 | 1051 | 0.80 | 84.7 | 428 |

### *b. Verification and secondary datasets testing*

The verification dataset was used to test the ability of models AVEIR, NIRVISQ and VISQ to predict rainfall using new station data during the development period (J74M78). Table 5 indicates that observed–predicted mean correlations are nearly identical to those

derived using the development dataset. Thus, the verification analysis indicates that the rainfall regression equations are generally applicable to regions of the tropical Pacific represented by the primary low-latitude islands.

To test model performance at higher latitudes, the secondary dataset was used (see section 2). Islands in this dataset were used only as qualitative indicators of rainfall because of their larger size and higher maximum elevations. Predicted-observed rainfall correlation for selected stations from this dataset are shown in Table 6. At the higher latitude islands near 25°N, 130°E and in the eastern Pacific, the VISQ model has nonsignificant correlations (the 0.05 significant level is $\sim > 0.38$), while both NIRVISQ and AVEIR have significant although not necessarily large correlations at all stations.

### c. *New temporal data testing*

The three models were also tested over two additional time periods, from January 1979–January 1980 and May 1980–December 1980. The former period was named J79J80, while the latter was named M80D80. The degradation of rainfall predictions during these latter time periods is shown in Table 7. Poorer predictions found in the later periods may be related to a number of factors, including the short periods of records and the different equatorial crossing times.

The equatorial crossing time problem was examined by using data from each time period and developing new statistical models. These models were unable to predict rainfall with greater accuracy during the J79J80 period, indicating that the original models' poorer predictions for this period may not have been caused by using equations derived with different equatorial crossing times. Models developed and tested using the M80D80 data did seem to have greater rainfall prediction skill. However, there were too few monthly observations in this period to make any firm statistical conclusions.

TABLE 6. Correlation comparisons ($r$) for different high-latitude island stations using data from the development, verification and secondary datasets.

| Island name | Location | VISQ $r$ | NIRVISQ $r$ | AVEIR $r$ |
|---|---|---|---|---|
| Midway | 28.2°N, 177.4°W | 0.54 | 0.58 | 0.59 |
| French F.S. | 23.9°N, 166.3°W | 0.70 | 0.70 | 0.87 |
| Ishigakijima | 24.3°N, 124.2°E | 0.27 | 0.32 | 0.28 |
| Miyakojima | 24.8°N, 125.3°E | −0.03 | 0.43 | 0.40 |
| Minamidaito | 25.8°N, 131.2°E | 0.28 | 0.57 | 0.56 |
| Lord Howe | 31.5°S, 159.1°E | 0.30 | 0.36 | 0.38 |
| Norfolk | 29.1°S, 167.9°E | 0.56 | 0.37 | 0.42 |
| Pitcairn | 25.0°S, 130.1°E | 0.54 | 0.43 | 0.54 |
| Easter | 27.2°S, 109.4°W | 0.55 | 0.57 | 0.56 |
| Juan-Fernandes | 33.6°S, 78.8°W | −0.09 | 0.59 | 0.64 |

TABLE 7. Comparison between models in different temporal periods. Data used in the comparisons consist of data from both development and verification datasets. Only island stations with rainfall data in all three time periods were used. The total period is derived by combining periods J74M78, J79J80 and M80D80 (see text).

| Model | Mean statistic | J74M78 | J79J80 | M80D80 | Total |
|---|---|---|---|---|---|
| VISQ | $r$ | 0.75 | 0.67 | 0.44 | 0.69 |
| | rmse (mm) | 89.7 | 109.5 | 94.9 | 96.1 |
| NIRVISQ | $r$ | 0.78 | 0.70 | 0.58 | 0.74 |
| | rmse (mm) | 83.1 | 95.2 | 83.9 | 87.2 |
| AVEIR | $r$ | 0.76 | 0.65 | 0.63 | 0.72 |
| | rmse (mm) | 88.3 | 105.2 | 83.6 | 92.7 |

## 5. Rainfall predictions

Figures 4a, b, c show the annual precipitation predicted by the VISQ, NIRVISQ and AVEIR models, formed from June 1974–May 1977 data. Taylor's (1973) estimate (T) of annual precipitation is shown for comparison in Fig. 4d. His estimate is based on measured island rainfall and mean cloud cover, as observed in visible mosiacs from the TIROS satellites, from which subjective estimates of tropical precipitation were made.

The most noticeable differences in Fig. 4 are between T or AVEIR and NIRVISQ and VISQ in the coastal regions of South America and Baja, California. In these regions T and the AVEIR model indicate minimum rainfall, whereas the VISQ and the NIRVISQ models suggest local maxima. Probably the persistent nonprecipitating stratus clouds in these regions reflect sufficient sunlight to give relatively large VISQ values and hence false rainfall estimates. Unfortunately, the lack of island rainfall data in this region prevents direct calibration of the satellite data.

The AVEIR, NIRVISQ and VISQ models appear to be in better agreement with each other and with T in regions of relatively high station density, such as the western equatorial Pacific. For example, near 5°N, 158°E, T shows a rainfall maximum exceeding 5000 mm. The three satellite models predict maximum values there of 3880, 3950 and 4030 mm for AVEIR, NIRVISQ and VISQ, respectively. Taylor (1973) indicates another maximum exceeding 5000 m near 11°S, 168°E. All of the satellite models show this maximum further to the northeast, centered over New Guinea.

A final feature worth noting in Figs. 4a–c is the greater apparent detail seen for VISQ and NIRVISQ when compared to AVEIR, suggesting that the AVEIR model may smooth rainfall features to a greater extent than those models using an albedo predictor.

## 6. Conclusions

This paper presents three new satellite data-based rainfall prediction models, referred to as AVEIR,

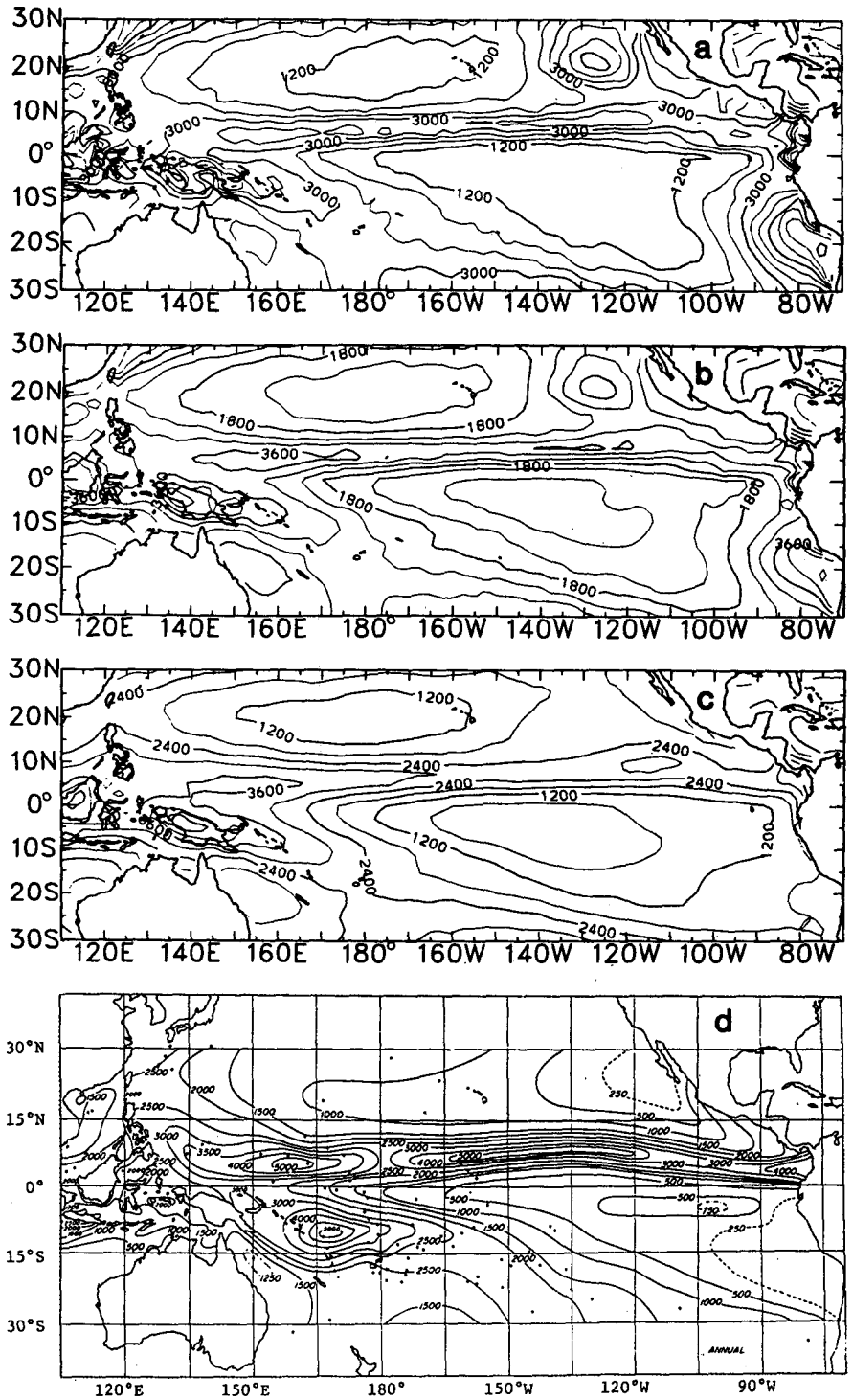


FIG. 4. Mean annual rainfall (mm $yr^{-1}$) for the Pacific basin predicted by (a) the AVEIR model, (b) NIRVISQ model, (c) VISQ model. (d) Distribution of the mean annual rainfall in millimeters (Taylor, 1973).

NIRVISQ and VISQ. These models are found to predict between 62% to 67% of the variance of 1051 station-months of hindcast rainfall data measured on small Pacific atolls.

Similar prediction accuracies are found when the rainfall models are used to predict rainfall on different low-latitude atolls during the development period (June 1974 through mid-March 1978). At stations poleward

of 20°, there is evidence that the rainfall models are less accurate than for stations equatorward of 20°. In particular, the albedo predictor model VISQ is unable to predict rainfall with any significant statistical accuracy (correlation) at two high-latitude island stations from the secondary dataset, whereas both AVEIR and NIRVISQ had significant correlations at those stations. These results are not conclusive since the secondary datasets includes islands with high elevations. However, they indicate that these rainfall models may be incapable of predicting rainfall from midlatitude synoptic storm systems.

There was also a decrease in predictive skills for all three models during the forecast time periods. The small number of monthly observations of these latter two periods (January 1979–January 1980 and May 1980–December 1980) hinders development of new statistical models for these periods or conclusive statements concerning the apparent causes.

All three models were shown to overpredict rainfall on relatively low mean rainfall islands and underpredict rainfall on relatively high mean rainfall islands. The rmse in the rainfall predictions was lowered between 6%–9% by predicting only rainfall anomalies.

Rainfall maps revealed that both VISQ and NIRVISQ had the undesirable effect of predicting much more rainfall in the eastern Pacific stratus regions than is expected from climatological studies, while the AVEIR model predicted reasonable rainfall amounts there. This suggests that rainfall prediction schemes using visible mosaics, such as Kilonsky and Ramage's (1976) method, may have a problem in distinguishing between stratus and rain-producing cumulus clouds unless some feature like texture is used to determine cloud type.

In regions of the western Pacific and ITCZ, both the NIRVISQ and VISQ models as well as the AVEIR model provide skillful rainfall estimates. The daily averaged infrared radiation model AVEIR appears to be the best overall model with reasonable rainfall predictive skill throughout the tropical Pacific including regions of intense convection activity and stratus clouds.

## APPENDIX A

**Island Rainfall Station**

Latitude, longitude and maximum elevation of island rainfall stations for the development stations (1–24), verification stations (25–44) and secondary stations (45–62).

| No. | Station | Latitude (°) | Longitude (°) | Max elevation (ft) | No. | Station | Latitude (°) | Longitude (°) | Max elevation (ft) |
|---|---|---|---|---|---|---|---|---|---|
| 1 | Willis | 16.3S | 150.0E | <30 | 32 | Kapingamarangi | 1.1N | 154.8E | 32 |
| 2 | Wake | 19.3N | 166.6E | 21 | 33 | Maiana | 1.0N | 173.0E | FA† |
| 3 | Eniwetok | 11.4N | 162.3E | 15 | 34 | Nukunau | 1.4S | 176.5E | FA |
| 4 | Kwajalein | 8.7N | 167.7E | 10 | 35 | Onotoa | 1.8S | 175.5E | FA |
| 5 | Majuro | 7.1N | 171.4E | 16 | 36 | Niutao | 6.1S | 177.3E | FA |
| 6 | Butaritari | 3.1N | 172.8E | 10 | 37 | Vaitupu | 7.5S | 178.7E | FA |
| 7 | Tarawa | 1.3N | 172.9E | 10 | 38 | Nukufetau | 8.0S | 178.5E | FA |
| 8 | Beru | 1.4S | 176.0E | 15 | 39 | Swain | 11.0S | 171.0W | FA |
| 9 | Arorae | 2.7S | 176.9E | 20 | 40 | Takaroa | 14.5S | 145.0W | 7 |
| 10 | Nanumea | 5.7S | 176.1W | 10 | 41 | Puka-Puka | 14.8S | 138.8W | FA |
| 11 | Nui | 7.3S | 176.2E | 10 | 42 | Palmerston | 18.1S | 163.2W | 15 |
| 12 | Funafuti | 8.5S | 179.2E | 15 | 43 | Hao | 18.1S | 141.0W | FA |
| 13 | Nukulaelae | 9.4S | 179.0E | FA | 44 | Hereheretue | 19.9S | 145.0W | FA |
| 14 | Midway | 28.2N | 177.4W | 43 | 45 | Ishigakijima | 54.3N | 124.2E | 1200 |
| 15 | French Frigate Shoals | 23.9N | 166.3W | 10 (221)* | 46 | Miyakojima | 24.8N | 125.3E | 370 |
| 16 | Johnston | 16.7N | 169.5W | 70 | 47 | Minamidaito | 55.8N | 131.2E | 200 |
| 17 | Canton | 2.8S | 171.7W | 10 | 48 | Yap | 9.5N | 138.1E | 585 |
| 18 | Atafu | 8.5S | 172.5W | 10 | 49 | Fanning | 3.6S | 159.0E | 10 |
| 19 | Washington | 4.5N | 160.4W | FA | 50 | Lord How | 31.5S | 159.1E | 5835 |
| 20 | Christmas | 2.0N | 157.4W | 10 | 51 | Norfolk | 59.1S | 167.9E | 1039 |
| 21 | Penrhyn | 9.0S | 158.1W | 10 | 52 | Lakemba | 18.2S | 178.4E | 720 |
| 22 | Rakahanga | 10.1S | 161.1W | 15 | 53 | Ono-I-Lau | 20.7S | 178.7E | 370 |
| 23 | Mopelia | 16.8S | 154.0W | 7 | 54 | Vavau | 18.7S | 174.0W | 610 |
| 24 | Tararoa | 14.5S | 145.0W | 7 | 55 | Nukualofa | 21.1S | 175.2W | 200 |
| 25 | Ulithi | 10.0N | 139.8E | <30 | 56 | Mangaia | 21.9S | 158.0W | 554 |
| 26 | Anguar | 6.9N | 134.1E | 60 | 57 | Mangareva | 23.1S | 134.9W | 1447 |
| 27 | Woleai | 7.4N | 143.9E | 36 | 58 | Rapa | 27.6S | 144.3W | 2077 |
| 28 | Satawan | 5.4N | 153.7E | 33 | 59 | Raoul | 29.3S | 177.9W | 1632 |
| 29 | Fanning | 3.8N | 159.4W | 10 | 60 | Pitcairn | 25.0S | 130.1W | 1000 |
| 30 | Little Makin | 3.3N | 174.0E | <10 | 61 | Easter | 27.2S | 109.4W | 1200 |
| 31 | Abaiang | 1.8N | 173.0E | FA | 62 | Juan Fernandes | 33.6S | 78.8W | 3005 |

* French Frigate Shoals is largely a flat tropical atoll, except on one side of the island complex where the maximum elevation rises to above 200 ft.

† FA denotes flat atoll with maximum elevation less than 30 m and exact elevation is unknown.

APPENDIX B

## Recalibration of Infrared Data

Gruber and Kreuger (1984) have proposed a recalibration of the infrared data used in this study to remove an observed positive bias. These recalibrated data are those which are available at the National Center for Atmospheric Research. To make more convenient use of this data with our proposed formulae we have developed revised regression equations corresponding to Eqs. 4 and 6:

model NIRVISQ:

$$R = 687.592 - 2.363\,(\mathrm{NIR}) + 2.774\,(\mathrm{VISQ}) \quad \text{(A4)}$$

model AVEIR:

$$R - 1591.721 - 5.658\,(\mathrm{AVEIR}) \quad \text{(A6)}$$

It may be noted that these equations are quite similar to the original. The correlations of predictions using Eqs. A4 and A6 with observation in the development set, corresponding to those in Table 4, are 0.83 and 0.80, respectively.

REFERENCES


Arkin, P. A., 1979: The relationship between fractional coverage of high cloud and rainfall accumulations during GATE over the B-scale array. *Mon. Wea. Rev.*, **107,** 1382–1387.

Barrett, E. C., and D. W. Martin, 1981: *The Use of Satellite Data in Rainfall Monitoring.* Academic Press, 340 pp.

Brooks, C. E. P., and N. Carruthers, 1953: *Handbook of Statistical Methods in Meteorology,* H. M. Stationery Off., 412 pp.

Daniel, C., and F. S. Wood, 1980: *Fitting Equations to Data: Computer Analysis of Multifactor Data.* Wiley, 458 pp.

Dorman, C. E., 1982: Comments on "Comparison of ocean and island rainfall in the tropical Pacific." *J. Appl. Meteor.*, **21,** 109–115.

Garcia, O., 1981: A comparison of two satellite rainfall estimates for GATE. *J. Appl. Meteor.*, **20,** 430–438.

Gruber, A., and J. S. Winston, 1978: Earth-atmosphere radiative heating based on NOAA scanning radiometer measurements. *Bull. Amer. Meteor. Soc.*, **59,** 1570–1573.

——, and A. F. Krueger, 1984: The status of the NOAA outgoing longwave radiation data set. *Bull. Amer. Meteor. Soc.*, **65,** 958–962.

Heddinghaus, T. R., and A. F. Krueger, 1981: Annual and interannual variations in outgoing longwave radiation over the tropics. *Mon. Wea. Rev.*, **109,** 1208–1218.

Horel, J. D., 1982: On the annual cycle of the tropical Pacific atmosphere and ocean. *Mon. Wea. Rev.*, **110,** 1863–1878.

Kilonsky, B. J., and C. S. Ramage, 1976: A technique for estimating tropical open-ocean rainfall from satellite observations. *J. Appl. Meteor.*, **15,** 972–975.

Lau, K.-M., and P. H. Chan, 1983: Short-term climate variability and atmospheric teleconnections from satellite-observed outgoing longwave radiation. Part I. Simultaneous relationships. *J. Atmos. Sci.*, **28,** 2735–2750.

Rao, M. S. V., V. Abbott III and J. S. Theon, 1976: Satellite-derived global oceanic rainfall atlas. NASA SP-410, 31 pp.

Riehl, H., and A. H. Miller, 1978: Differences between morning and evening temperatures of cloud tops over tropical continents and oceans. *Quart. J. Roy. Meteor. Soc.*, **104,** 757–764.

Short, D. A., and J. M. Wallace, 1980: Satellite-inferred morning-to-evening cloudiness changes. *Mon. Wea. Rev.*, **108,** 1160–1169.

Stout, J. E., D. W. Martin and D. N. Sikdar, 1979: Estimating GATE rainfall with geosynchronous satellite images. *Mon. Wea. Rev.*, **107,** 585–598.

Taylor, R. C., 1973: An Atlas of Pacific Island Rainfall. Hawaii Institute of Geophysics Data Report No. 25. [Available from the Dept. of Meteorology, University of Hawaii.]

Weisberg, S., 1980: *Applied Linear Regression.* Wiley, 283 pp.

Woodley, W. L., C. G. Griffith, J. S. Griffin and S. C. Stromatt, 1980: The influence of GATE convective rainfall from SMS-1 imagery. *J. Appl. Meteor.*, **19,** 388–408.